

Conceptual framework for performing simultaneous fold and sequence optimization in multi-scale protein modeling

István Kolossváry^{1, 2,*}

¹*Department of Chemistry, Budapest University of Technology and Economics,
H-1111 Budapest, Hungary*

²*BIOKOL Research, LLC, Madison, New Jersey 07940, USA*

*Correspondence: Istvan@Kolossvary.hu

PACS number(s): 87.15.Cc, 02.60.Pn, 87.15.A-

We present a dual optimization concept of predicting optimal sequences as well as optimal folds of off-lattice protein models in the context of multi-scale modeling. We validate the utility of the recently introduced hidden-force Monte Carlo optimization algorithm by finding significantly lower energy folds for minimalist and detailed protein models than previously reported. Further, we also find the protein sequence that yields the lowest energy fold amongst all sequences for a given chain length and residue mixture. In particular, for protein models with a binary sequence, we show that the sequence-optimized folds form more compact cores than the lowest energy folds of the historically fixed, Fibonacci-series sequences of chain lengths of 13, 21, 34, 55, and 89. We then extend our search algorithm to use UNRES, one of the leading united-residue protein force fields. Our combined fold and sequence optimization on three test proteins reveal an inherent bias in UNRES favoring alpha helical structures even when secondary structure prediction clearly suggests only beta sheets besides random coil, and virtually no helices. One test in particular, a triple-stranded antiparallel beta-sheet protein domain, demonstrates that by permutations of its sequence UNRES re-folds this structure into a perfect alpha helix but, in fact, the helix is just an artefact of the force field, the structure quickly unfolds in all-atom state-of-the-art molecular dynamics simulation.

I. INTRODUCTION

We recently introduced the hidden-force algorithm (HFA), a global Monte Carlo optimization method and used it to predict low-energy binary Lennard-Jones (BLJ) cluster configurations [1]. In this communication, we apply HFA to find the optimal fold of simple and detailed protein models. Further, we also find the protein sequence that yields the lowest energy fold amongst all sequences for a given chain length and residue mixture. In particular, we study protein AB (PAB) models [2, 3]. These have close similarity to BLJ models. Despite their minimalism, PAB models mimic a basic feature of protein folding—the formation of a hydrophobic core. Similar to BLJ models PAB models consist of only two types of residues, denoted A and B. The interaction energy between two A residues (AA interaction) is twice as strong as AB or BB interactions to promote core formation. The interaction potential has a pseudo Lennard-Jones form and the total potential energy includes angle-bending and torsion terms to account for local interactions. Historically, PAB models use a Fibonacci series sequence protein with chain lengths of 13, 21, 34, 55, and 89 [4, 5]. At first, we revisit the Fibonacci sequences and find that much lower energy folds exist than previously reported. Moreover, the new putative global minima show topological features qualitatively different from real proteins. The new low-energy folds are deeply knotted indicative of a flaw in the PAB model. Simplifying the local interaction terms introduced to extend the PAB model to three dimensions [3], we obtain new realistic low-energy folds without knots. Using this simplified potential we use HFA optimization to find non-Fibonacci sequences that fold into still lower energy structures with more compact cores comprised of A residues.

We then apply HFA optimization to six test proteins using UNRES, one of the leading united-residue force fields [6, 7, 8] that has been highly successful in the past fifteen years of CASP competition (Critical Assessment of protein Structure Prediction [9]) [10]. First, as a validation of HFA on this sophisticated two-bead model, we compare our global minima to those found by UNRES/CSA [11] and for five out of the six proteins find lower energy folds. We also find, however, that these new global minima all represent slightly unfolded structures, which is indicative of a flaw in the force field and/or a flaw in the concept of locating the global minimum of a potential energy function as a means to identify the global minimum free-energy

structure/fold. Furthermore, we probe the UNRES force field by once again applying sequence optimization in order to find sequences that fold into still lower energy structures, and find that UNRES has a strong tendency to fold sequences into alpha helices. One test in particular, a WW domain (1E0L), which is the smallest monomeric triple-stranded antiparallel beta-sheet protein domain, demonstrates that by permutations of its sequence HFA/UNRES re-folds this structure into a perfect alpha helix.

II. MODEL AND ALGORITHMIC DETAILS

PAB models are one of the minimalist protein models [12]. We used the model by Irbäck *et. al* [3], a well-studied three-dimensional extension of the original two-dimensional PAB model by Stillinger *et. al* [2]. In this model proteins consist of two types of residues, A and B. Each residue represents a C α atom. The C α -C α bonds are set to unit length and the potential energy is:

$$E = -\kappa_1 \sum_{i=1}^{N-2} \cos C\alpha_{i,i+1,i+2} - \kappa_2 \sum_{i=1}^{N-3} \cos C\alpha_{i,i+1,i+2,i+3} + \sum_{i=1}^{N-2} \sum_{j=i+2}^N 4\varepsilon(\sigma_i, \sigma_j) \left(\frac{1}{r_{ij}^{12}} - \frac{1}{r_{ij}^6} \right). \quad \text{Eq. 1}$$

The first two sums represent local interactions as angle-bending or torsion energies, involving three or four consecutive C α atoms, respectively. The last double sum is a pseudo Lennard-Jones (LJ) potential representing long-range interactions. N is the number of residues, r_{ij} is the distance between two residues, $\varepsilon(\sigma_i, \sigma_j)$ is the residue pair-specific LJ well-minimum depth, and κ_1 and κ_2 are empirical parameters determined by Monte Carlo simulations to reproduce qualitatively C α angle and torsion distributions of proteins in the Protein Data Bank (PDB) [3]. We used $\kappa_1 = -1$ and $\kappa_2 = 0.5$. $\varepsilon(\sigma_i, \sigma_j)$ favor the formation of a core of A residues analogous to the hydrophobic core of real proteins: $\varepsilon(A, A) = 1$ and $\varepsilon(A, B) = \varepsilon(B, B) = 0.5$. LJ interactions between adjacent residues are excluded. In lieu of constraints we add strong harmonic distance terms to keep C α -C α bond lengths at unity and flat-bottom angle-bending terms to disallow near linear C α -C α -C α bond angles (within two degrees). Linear bond angles cause a catastrophic physical divergence in the torsion term of the PAB model.

The UNRES model is a sophisticated two-bead representation of the polypeptide chain. Each amino acid residue is represented by two interaction centers, one is the halfway point between

two consecutive C α atoms (the C α atoms themselves serve only as geometric reference points), and the other interaction center is the center of mass of the side chain that is modeled as an ellipsoid with two rotational degrees of freedom with respect to the backbone. Backbone flexibility itself is allowed by varying virtual-bond angles and virtual-bond dihedral angles along three or four C α atoms, respectively. The UNRES force field includes numerous bonded and non-bonded terms as well as implicit contributions from the interaction of the side chain with the solvent [6, 7, 8] and has been parameterized utilizing the so-called hierarchical design of the potential-energy landscape employing multiple training proteins simultaneously [13].

The hidden-force algorithm [1] exploits that, though the gradient components of an additive potential sum to zero at a local minimum, each component's magnitude is generally nonzero. Disrupting this network of opposing forces (negative of the gradient) can result in the collective rearrangement of cluster atoms. Using a tug-of-war analogy to describe the basic HFA move, some players (atoms) simultaneously drop their ropes (drop their contributions to the potential). The remaining players then rearrange due to their net nonzero tugging and reach a partial impasse. Then the dropouts resume tugging until a new total impasse is achieved. There is no guarantee that the resulting cluster configuration will be lower in energy than the starting configuration, but we found HFA to be an exceptionally successful move set in a Monte Carlo cluster minimization. HFA trial configurations are highly dependent on the starting configurations since the moves are driven by forces already present—making the HFA Monte Carlo search non-Markovian.

Algorithmically, PAB models can be treated similar to BLJ clusters with slightly different LJ terms and additional geometric constraints favoring protein like chains. We used the same algorithm and software described in detail in [1] with two notable differences: (1) when the basic HFA move is applied to a given local minimum-energy configuration, only the pseudo LJ terms are dropped; the remaining terms stay in effect to preserve the chain geometry. (2) Single or multiple mutations are utilized by swapping the types of randomly selected residues rather than flipping the type of a single residue at a time, in order to keep the composition fixed while varying the sequence. A BLJ cluster of fixed size is fully determined by its A/B composition, but PAB models also depend on the *sequence* of the residues. Therefore, while swapping A and B particles in a BLJ cluster will not change its identity, swapping A and B residues in a PAB protein will be a mutation. Further, in [1], we found the optimal A/B composition of a BLJ cluster of fixed size with lowest energy. For PAB models, the optimal A/B composition is trivial, a sequence of all A

residues (AA interactions are stronger than AB or BB interactions). The more interesting and challenging mutation study we carry out keeps the A/B composition fixed and optimizes over sequences to find the lowest energy fold.

Employment of the UNRES model requires further significant but straightforward changes in the HFA algorithm with respect to how it is utilized with PAB models. (1) When the basic HFA move is applied, instead of simply dropping the non-bonded interactions, the selected residue is temporarily mutated into GLY, and it keeps all of its interactions. (2) Since UNRES is a two-bead model, every local minimization step is combined with side chain optimization along the full length of the polypeptide chain. Moreover, akin to the PAB studies we mutate the UNRES models by swapping one or more pairs of residues keeping the overall residue composition fixed and optimize over sequences to find the lowest energy fold. It should be noted, however, that while such residue swaps readily allow direct comparison of the energies of different sequence mutants in the minimal PAB model, this is not trivial with UNRES. Similar to all-atom molecular mechanics force fields, UNRES energy is not absolute and, therefore, energies of two different molecules are generally not comparable. Nonetheless, when comparing the energies of two different peptides with the same residue composition, but subject to single or multiple residue swaps and altogether having different residue sequences, is an exception. The energies of such peptides (we shall call them permutation isomers) are indeed comparable in any molecular mechanics force field including UNRES devoid of sequence dependent terms. UNRES does have the built-in capability of employing sequence dependent terms, but the current parameterization omits them.

III. RESULTS AND DISCUSSION

To test HFA against existing optimization methods for PAB models, we run HFA searches on Fibonacci sequences in [Table I](#) and compare our putative global minimum-energy folds with those found in [\[4, 5\]](#). [Table I](#) clearly demonstrates that HFA Monte Carlo search is efficient searching the fold space of PAB models. The difference in energy does not carry information about structural differences, though. Direct comparison was, unfortunately, not possible because the coordinates of the structures reported in [\[4, 5\]](#) were not published. Nonetheless, based on the visualizations in [\[4, 5\]](#), [FIG. 1](#) clearly shows that our new minima belong to a different topological

class indicative of a flaw in PAB models. With the exception of S_13, which is simply too short and S_21 that forms a simple trefoil knot (one end of the chain folding back through a loop), every other fold is deeply knotted (coordinates are listed in the Supplementary Material). Knotted protein structures occur naturally [14, 15], however, this level of knot formation cannot be found in the PDB [16]. With $\kappa_1 = -1$ and $\kappa_2 = 0.5$ [3], the simple cosine terms favor a 180 degree bond angle and a zero degree torsion angle. In real proteins, the bond angle distribution has a well-defined structure and bond angles strictly fall within the range of 85-145 degrees [3]. Torsion angles, on the other hand, are more uniform; there are no disallowed values. Nevertheless, zero degree torsion angles are rare. Eq. 1 represents an additive potential and even though the PAB models will always be frustrated in three dimensions, we can expect that at or close to the global minimum many individual energy terms will be close to their minimum values. This is exactly what we can see in FIG. 1; numerous bond angles are close to 180 degrees (kept away from exact linearity by the flat bottom angle-bending term) and numerous torsion angles are very close to zero degrees. This is the geometrical basis for forming knots in the ground state, never seen in real proteins.

Table I. Energies of the new putative global minima listed in ϵ units, found by HFA for five Fibonacci sequences. The * operator in the Sequence column means concatenation. The previously reported energies were taken from [4, 5].

Model identifier with chain length	Sequence	Lowest energy [ϵ] previously reported	Putative global minimum energy [ϵ]
S_13	ABBABBABABBAB	-26.507	-27.171
S_21	BABABBAB * S_13	-52.934	-56.409
S_34	S_13 * S_21	-98.357	-106.115
S_55	S_21 * S_34	-176.691	-190.579
S_89	S_34 * S_55	-311.614	-325.578

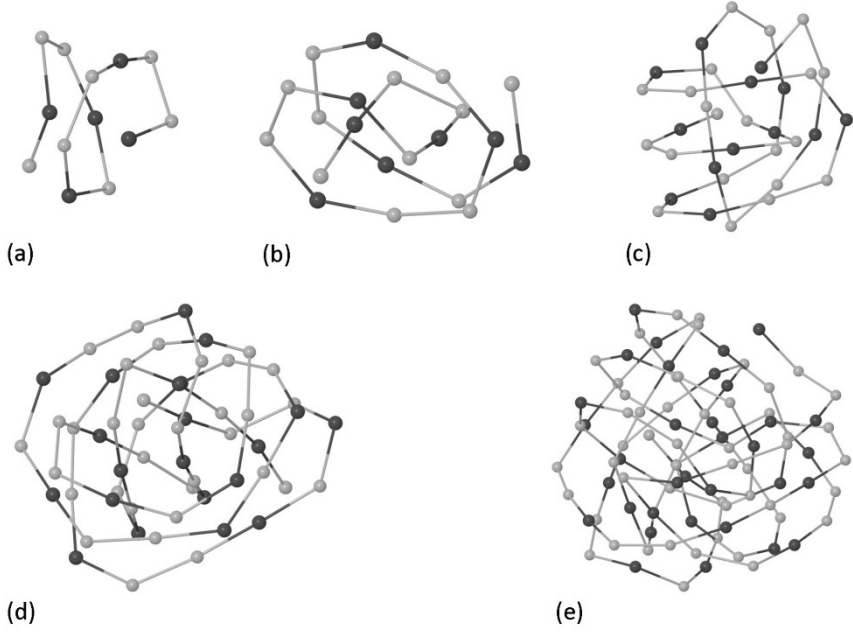


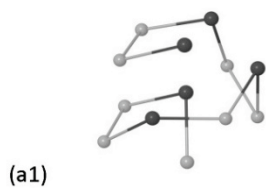
FIG. 1. Putative global minimum-energy folds found for 5 Fibonacci sequences using the potential in Eq. 1. Dark balls represent type A (“hydrophobic”) residues and light grey balls are type B residues. Sequences and energies are given in Table I. (a) S_13, (b) S_21, (c) S_34, (d) S_55, and (e) S_89.

Ideally, more sophisticated potentials should be derived from the actual $\text{C}\alpha$ bond angles and torsion angles found in the PDB via, e.g., the Boltzmann inversion method [12]. Keeping with the minimalist spirit of PAB models, however, we drop the angle-bending and torsion terms altogether, but we add a flat-bottom harmonic angle term that disallows $\text{Ca}-\text{Ca}-\text{Ca}$ angles outside the 85-145 degree range. Using this potential we find that the Fibonacci sequences fold into globular structures with no tendency to form knots, and with a “hydrophobic” core. We then carried out sequence optimization using this potential. The left hand side of FIG. 2 shows the putative global minima found for the five Fibonacci sequences and the right hand side shows the lowest energy folds after sequence mutations were applied to the Fibonacci sequences (coordinates are available in the Supplementary Material). Visual inspection confirms the simplified PAB

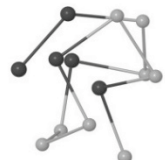
model yields compact folds with a clear core and no knots. The cores are more compact in the mutated sequences, which is quantified in [Table II](#) by the radius of gyration of the core (type A) residues. [Table II](#) also lists the energy drop after sequence optimization with respect to the putative global minimum energy of the Fibonacci sequence.

[Table II](#). Fold optimization via sequence mutation. Energy drop and radius of gyration of the “hydrophobic” core formed by the type A residues. Energy is computed with the LJ-only potential (see text). The optimal sequences, coordinates, and absolute energies are listed in the Supplementary Material.

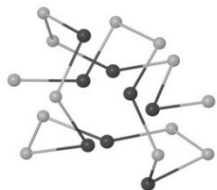
Model identifier with chain length	Energy drop [ϵ] relative to Fibonacci sequence global min.	Radius of gyration of the core in Fibonacci sequence global min.	Radius of gyration of the core in optimal- sequence global min.
S_13	-0.346	0.203	0.156
S_21	-1.369	0.288	0.223
S_34	-2.748	0.336	0.281
S_55	-9.074	0.371	0.327
S_89	-18.576	0.460	0.365



(a1)



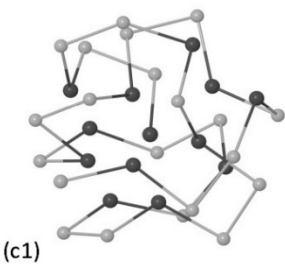
(a2)



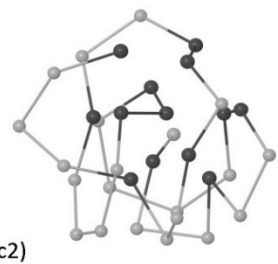
(b1)



(b2)



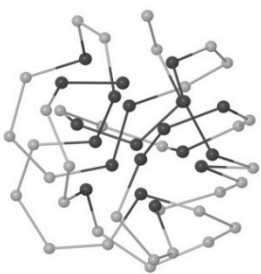
(c1)



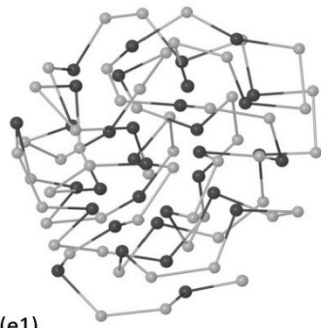
(c2)



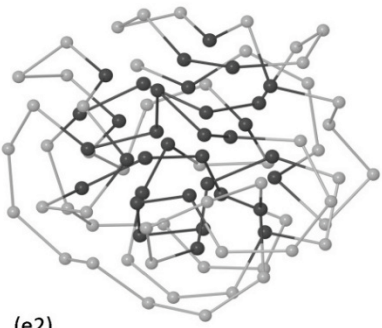
(d1)



(d2)



(e1)



(e2)

FIG. 2. Putative global minimum-energy folds using the simplified LJ-only potential (see text). On the left hand side the Fibonacci sequences are shown and on the right hand side the optimal folds are displayed that were found after sequence optimization. Dark balls represent type A (“hydrophobic”) residues and light grey balls are type B residues. The optimal sequences, coordinates, and energies are listed in the Supplementary Material. (a1, a2) S_13, (b1, b2) S_21, (c1, c2) S_34, (d1, d2) S_55, and (e1, e2) S_89.

To further test HFA against UNRES’ native conformational space annealing (CSA) [11] global-optimization method, we run HFA searches on six test proteins (1BDD, 1GAB, 1LQ7, 1CLB, 1E0G, and 1IGD) that were essential in parameterizing UNRES. Among the force field options in UNRES we employ 4P (parameterized using four training proteins simultaneously) that is most adequate for small proteins of any fold including alpha, beta, and alpha/beta [13, 17]. **Table III** demonstrates that HFA Monte Carlo search is also efficient searching the fold space of sophisticated UNRES models. Similar to the PAB study, the difference in energy itself does not carry information about structural differences and direct comparison was, unfortunately, not possible because the coordinates of the structures reported in [18] were not published with the exception of 1IGD for which the complete CSA results are available in the UNRES download kit [19]. Nevertheless, the results point to noteworthy anomalies. Similar energies and similar RMS distances found with 1BDD, 1CLB, and 1E0G suggest that CSA and HFA searches located the same ground state folds for these chains. Moreover one could even argue that since the HFA ground state for 1GAB is significantly lower in energy than the lowest lying CSA structure and at the same time the HFA fold is 0.3 Å closer to the experimental structure in C-alpha RMS distance than the CSA minimum; lowering the energy might have the general effect of actually getting closer to the native structure, and thereby providing strong support for the force field. However, the two remaining proteins in **Table III** crush such hopes. HFA generated a fold for 1LQ7 that has virtually the same energy as the CSA ground state, yet the HFA fold is more than 4 Å farther away from the experimental structure than the quite accurate CSA minimum. 1IGD yields an even more negative result where the HFA ground state is, again, over 4 Å farther away than the CSA minimum, but the HFA fold has significantly (11 kcal/mol) lower energy. The C-alpha RMS distance between the CSA and HFA folds is 8.8 Å and visual inspection clearly shows that in the HFA ground state the alpha helix and both antiparallel beta strands start to unfold. The C-alpha

coordinates of all six of the HFA putative global minimum-energy structures are listed in the Supplementary Material.

Table III. UNRES/4P energies of the lowest lying structures of six test proteins and their C-alpha RMS distances from the corresponding experimental structure found by CSA [18] and HFA, respectively. The number of residues are shown in parentheses. The C-alpha coordinates of the HFA putative global minimum-energy structures are listed in the Supplementary Material.

PDB ID	CSA glob. min. energy [kcal/mol]	HFA glob. min. energy [kcal/mol]	CSA RMSD to exp. struct. [Å]	HFA RMSD to exp. struct. [Å]
1BDD (46)	-597	-601	5.5	5.6
1GAB (47)	-669	-681	2.9	2.6
1LQ7 (67)	-937	-937	2.3	6.6
1CLB (75)	-1053	-1054	5.1	5.2
1E0G (48)	-632	-634	4.1	4.3
1IGD (61)	-741	-752	5.6	9.9

We conclude our UNRES tests with running HFA sequence optimization on three proteins to learn more about the force field. We choose a pure alpha protein 1BDD, a mixed alpha/beta protein 1IGD, and a pure beta mini protein 1E0L (28 residues), which is the smallest monomeric triple-stranded antiparallel beta-sheet protein domain. We want to see if sequence optimization can provide stable folds lower in energy than those of the native sequence/fold and whether we can draw any general conclusions about UNRES in this regard as we do with the modified PAB model above. Sequence optimization involves periodically swapping pairs of residues followed by HFA fold search and thereby exploring the sequence space of permutation isomers. As noted above, UNRES energy is not absolute but energies of permutation isomers are readily comparable.

FIG. 3, FIG. 4, and FIG. 5 give vivid visual insight and to put it bluntly; everything folds into a helix. The left hand side of the figures show the HFA ground state structure of the native sequence (rainbow colors from red N-terminus to purple C-terminus) superposed on the experimental structure shown in gray and the right hand side presents the result of sequence optimization. The figures also include the native sequence vs. optimized sequence and the associated energy drop. The evident qualitative statement that can be drawn from the figures is that sequence optimization re-folds all three native structures into helical structures with significant energy stabilization. Moreover, as shown by explicit tube representation, PRO residues are either pushed out the termini or break the alpha helices in the interior of the chain as generally seen in real protein structures, and GLY residues tend to shift to flexible coil segments. One would of course be tempted to draw physical conjectures based on the sequence optimization data, but further analysis makes it clear that folding into these predominantly alpha helical structures is, in fact, just a serious artefact of the UNRES force field. We provide two types of evidence.

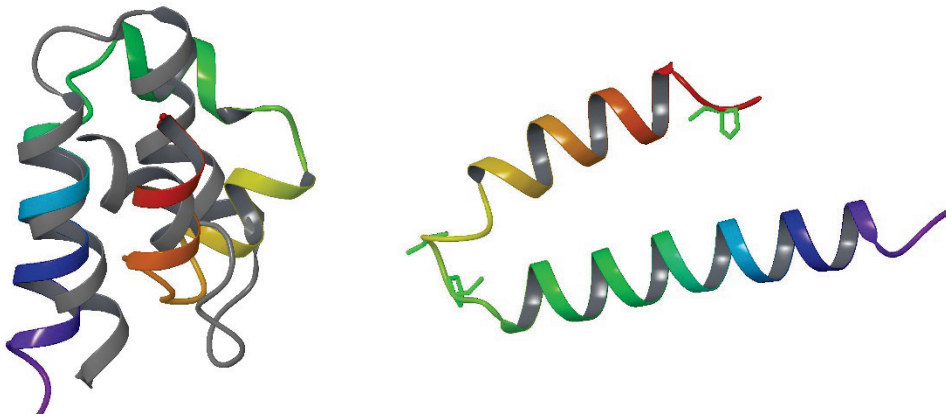


FIG. 3. Ground state sequence-permutation isomer of 1BDD. Energy drop 21 kcal/mol. See text for details. First row shows the native sequence and the second row shows the energy-optimized sequence below:

QQNAFYEILHLPNLNEEQRNGFIQSLKDDPSQSANLLAEAKKLNDA
SPAETYKKEALDQAIQLSGDPESNFIKLQEALLLFNHNQQALRNNNDN

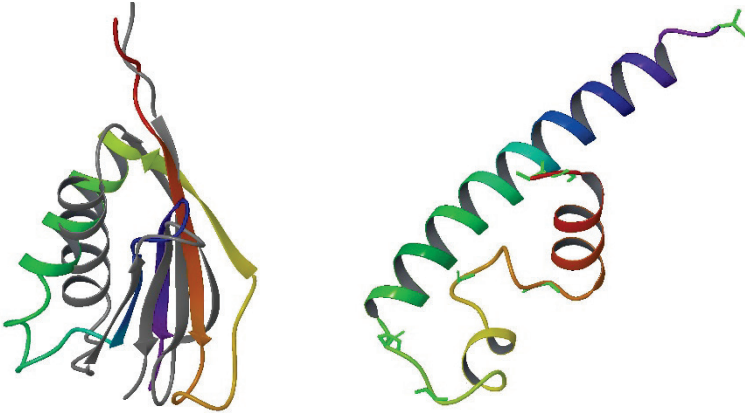


FIG. 4. Ground state sequence-permutation isomer of 1IGD. Energy drop 41 kcal/mol. See text for details. First row shows the native sequence and the second row shows the energy-optimized sequence below:

GMTPAVTTYKLVINGKTLKGETTKAVDAETAEKAFKQYANDNGVDGVWTYDDATKTFTVTEG
GGEAAVTMWANVGEVDGTYKFTDKADGKPATDTNTETANYVVQFILVAKKLTDYETTKTKG

First, secondary structure prediction performed on the optimized sequences by multiple trusted web servers [20] provides no evidence for helical segments in either the 1IGD or the 1E0L ground state permutation isomers; the predictions are all beta and random coils (except for a tiny alpha contribution in 1IGD). Not surprisingly, however, 1BDD itself being an all-alpha protein, retains its alpha character after sequence optimization. Second, the extreme case of 1E0L where sequence optimization results in re-folding a pure triple-stranded antiparallel beta-sheet into a pure alpha helical structure, pleads for more accurate calculations. Here we employ multi-scale modeling by (i) generating the full backbone structure from the C-alpha coordinates [21], (ii) applying highly accurate side chain prediction using SCWRL4 [22], and finally (iii) running all-atom molecular dynamics (MD) simulation with explicit solvent. We carry out the MD simulation with Desmond [23] running on a NVIDIA GeForce GTX 780 graphics processor and using a simulation protocol that has proven highly successful in folding numerous small proteins [24]. The length of the MD simulation is 150 ns and the MPEG video file (70 MB) is available upon request. The trajectory provides vivid graphical evidence that the all-alpha UNRES ground-state sequence-permutation isomer of 1E0L is not stable at all, it entirely unfolds in less than 10 ns and remains in a highly volatile, flexible and somewhat U-shaped random coil configuration for the rest of the simulation.

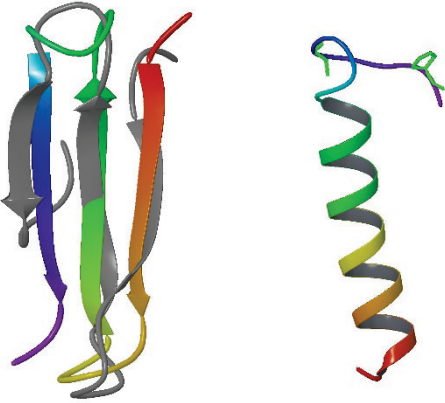


FIG. 5. Ground state sequence-permutation isomer of 1E0L. Energy drop 45 kcal/mol. See text for details. First row shows the native sequence and the second row shows the energy-optimized sequence below:

SEWTEYKTADGKYYYYNNRTLESTWEKP
NRTETYLSNTETYEKKWTWADGSKPY

IV. SUMMARY AND PERSPECTIVE

In this communication, we propose a dual concept for the global optimization of off-lattice protein models predicting optimal sequences as well as optimal folds and embed our approach in multi-scale modeling. Using hidden-force Monte Carlo optimization we find the optimal fold of simple and detailed protein models. Further, we also find the protein sequence that yields the lowest energy fold amongst all sequences for a given chain length and residue mixture. We then generate an all-atom model and run state-of-the-art MD simulation. In particular, we find that with a simplified potential, binary protein AB models fold into globular, compact structures with no tendency to form knots, and with a “hydrophobic” core. Historically, these models use a Fibonacci series sequence protein with chain lengths of 13, 21, 34, 55, and 89. We show that sequence optimization yields non-Fibonacci sequences that fold into still lower energy structures with more compact cores than the original Fibonacci sequences. We extend our investigation to study real proteins using the sophisticated UNRES model and find via sequence optimization and all-atom MD simulation that UNRES inherently favors helical structures.

We demonstrate that our methodology is applicable to detailed protein models, fits well within multi-scale modeling, and ultimately may aid de novo protein design by yielding novel folds. However, we also demonstrate that further improvements in force fields are needed before sequence optimization could become a reliable tool for proteins in general, and for the moment our research focus stays within the realm of all-alpha proteins, studying sequences that afford stable folds—whether native or non-native.

Acknowledgement. I am indebted to Adam Liwo for instrumental assistance with UNRES.

-
- [1] I. Kolossváry and K. J. Bowers, [Phys. Rev. E **82**, 056711 \(2010\)](#).
 - [2] F. H. Stillinger, T. Head-Gordon, and C. L. Hirshfeld, [Phys. Rev. E **48**, 1469 \(1993\)](#).
 - [3] A. Irbäck, C. Peterson, F. Potthast, and O. Sommelius, [J. Chem. Phys. **107**, 273 \(1997\)](#).
 - [4] J. Lee, K. Joo, S.-Y. Kim, and J. Lee, [J. Comput. Chem. **29**, 2479 \(2008\)](#).
 - [5] C. Zhang and J. Ma, [J. Chem. Phys. **130**, 194112 \(2009\)](#).
 - [6] A. Liwo, S. Oldziej, M. R. Pincus, R. J. Wawak, S. Rackovsky, and H. A. Scheraga, [J. Comput. Chem. **18**, 849 \(1997\)](#).
 - [7] A. Liwo, M. R. Pincus, R. J. Wawak, S. Rackovsky, S. Oldziej, and H. A. Scheraga, [J. Comput. Chem. **18**, 874 \(1997\)](#).
 - [8] A. Liwo, R. Kazmierkiewicz, C. Czaplewski, M. Groth, S. Oldziej, R. J. Wawak, S. Rackovsky, M. R. Pincus, and H.A. Scheraga, [J. Comput. Chem. **19**, 259 \(1998\)](#).
 - [9] <http://predictioncenter.org>.
 - [10] Y. He, M. A. Mozolewska, P. Krupa, A. K. Sieradzan, T. K. Wirecki, A. Liwo, K. Kachlishvili, S. Rackovsky, D. Jagiela, R. Slusarz, C. R. Czaplewski, S. Oldziej, and H. A. Scheraga, [Proc Natl Acad Sci U S A **110**, 14936 \(2013\)](#).
 - [11] J. Lee, D. R. Ripoll, C. Czaplewski, J. Pillardy, W. J. Wedemeyer, and H. A. Scheraga, [J. Phys. Chem. B **105**, 7291 \(2001\)](#).
 - [12] V. Tozzini, [Quart. Rev. Biophys. **43**, 333 \(2010\)](#).
 - [13] S. Oldziej, J. Lagiewka, A. Liwo, C. Czaplewski, M. Chinchio, M. Nalias, and H. A. Scheraga, [J. Phys. Chem. B **108**, 16950 \(2004\)](#).
 - [14] W. L. Taylor, [Nature **406**, 916 \(2000\)](#).
 - [15] W. L. Taylor, [Comput. Biol. Chem. **31**, 151 \(2007\)](#).
 - [16] <http://www.rcsb.org>.
 - [17] <http://www.unres.pl/unres>, Chapter 7 (Force Fields).

-
- [18] A. Liwo, M. Khalili, and H. A. Scheraga, [Proc Natl Acad Sci U S A **102**, 2362 \(2005\)](#).
 - [19] <http://www.unres.pl/downloads>, in the directory examples/CSA/4P/CSA/.
 - [20] <http://expasy.org/resources/search/keywords:secondary%20structure%20prediction>.
 - [21] M. Levitt and J. Geer, [J. Mol. Biol **114**, 181 \(1977\)](#).
 - [22] G. G. Krivov, M. V. Shapovalov, and R. L. Jr. Dunbrack, [Proteins **77**, 778 \(2009\)](#).
 - [23] K. J. Bowers, E. Chow, H. Xu, R. O. Dror, M. P. Eastwood, B. A. Gregersen, I. Kolossváry, J. L. Klepeis, M. A. Moraes, F. D. Sacerdoti, J. K. Salmon, Y. Shan, and D. E. Shaw, [Proceedings of the ACM/IEEE Conference on Supercomputing \(SC06\)](#), New York, NY: IEEE, (2006).
 - [24] K. Lindorff-Larsen, S. Piana1, R. O. Dror, and D. E. Shaw, [Science **334**, 517 \(2011\)](#)
Supporting Online Material.

Title: Conceptual framework for performing simultaneous fold and sequence optimization in multi-scale protein modeling

Author: Istvan Kolossvary

Description:

List of coordinates, sequences, and energies of putative global minimum folds of PAB and UNRES models. The coordinates are Cartesian coordinates. The sequence is identified by the residue type A or B in the first column. Energies are absolute energies in epsilon units. The first 5 models were computed with the potential in Eq. 1. The other 5 models were computed with the simplified potential including the pseudo Lennard-Jones potential, the bond length restraint and the flat-bottom angle bending constraint to keep the Calpha-Calpha-Calpha bond angles within the 85-145 degree range. The UNRES protein models below are represented by their C-alpha atoms listed in PDB format. The energy is UNRES/4P.

S_13 Fibonacci sequence global minimum energy computed by Eq. 1 =
-27.171382

A	-2.210729	-0.766557	0.859473
B	-1.468936	-0.515469	1.481321
B	-1.125457	0.413991	1.346684
A	-2.015611	0.307761	0.903583
B	-2.875024	0.042923	0.466239
B	-2.923165	-0.824726	-0.028602
A	-2.104003	-1.398285	-0.026841
B	-1.292453	-1.270099	0.543208
A	-1.100612	-0.289674	0.498904
B	-1.256479	0.656395	0.214902
B	-2.203998	0.733500	-0.095357
A	-1.998733	-0.244823	-0.122725
B	-1.256899	-0.823838	-0.460991

S_21 Fibonacci sequence global minimum energy computed by Eq. 1 =
-56.408990

B	-3.502088	-2.347106	-2.580986
A	-3.633583	-3.070794	-1.903502
B	-3.182330	-2.964804	-1.017422
A	-2.558379	-2.207111	-0.826145
B	-1.942815	-1.419028	-0.828706
B	-1.631517	-1.022569	-1.692370
A	-1.917468	-1.469613	-2.539947
B	-2.396659	-2.287089	-2.859494
A	-2.809866	-3.188090	-2.727356
B	-2.658749	-3.616882	-1.836679
B	-2.088394	-3.137323	-1.169805
A	-1.497975	-2.495615	-0.680298
B	-0.926488	-1.760655	-1.045314
B	-0.814412	-1.662030	-2.034107
A	-1.235498	-2.340732	-2.635811
B	-1.870827	-3.002000	-2.236963
A	-2.685908	-2.555420	-1.867897
B	-3.446519	-2.008019	-1.518868
B	-2.589028	-1.522775	-1.689879

A	-1.763180	-2.085958	-1.661572
B	-0.995117	-2.724986	-1.620079

S_34 Fibonacci sequence global minimum energy computed by Eq. 1 =
-106.115214

A	-0.054962	2.229487	-0.900343
B	-0.853011	2.143012	-1.496697
B	-0.951238	1.732429	-0.590181
A	-0.524775	1.446744	0.268022
B	0.330605	1.385370	0.782374
B	1.265892	1.429216	1.133538
A	1.199972	1.905059	0.256483
B	0.995707	2.354906	-0.612946
A	0.707322	2.800658	-1.460375
B	-0.237086	3.129292	-1.450697
B	-0.878686	2.917563	-0.713459
A	-0.848802	2.520503	0.203846
B	-0.411806	2.204694	1.046045
B	0.565968	2.364524	1.181737
A	1.553768	2.506594	1.117971
B	2.284360	2.032034	0.627028
A	2.006677	1.145438	0.257113
B	1.079417	0.771783	0.233288
B	0.127003	0.470460	0.187356
A	-0.495836	0.717894	-0.554834
B	-0.200073	1.245807	-1.350967
A	0.708342	1.655607	-1.433690
B	1.614781	2.075060	-1.482927
B	1.824123	2.954070	-1.054539
A	1.063933	3.448186	-0.632687
B	0.147975	3.147931	-0.366482
B	0.176094	2.278401	0.126597
A	0.388799	1.417582	-0.335729
B	0.682145	0.618698	-0.860826
A	1.419258	1.273341	-0.693175
B	2.059386	2.006824	-0.464622
B	1.809237	2.833024	0.040171
A	0.893430	3.031008	0.389595
B	-0.039220	3.183399	0.716612

S_55 Fibonacci sequence global minimum energy computed by Eq. 1 =
-190.579174

B	-1.048644	-1.434770	-2.612892
A	-0.857230	-1.125885	-1.681255
B	-0.596707	-0.675295	-0.827388
A	-0.290393	-0.155407	-0.029967
B	0.110010	0.484079	0.626335
B	0.162770	0.776914	-0.328370
A	0.162639	0.678281	-1.323493
B	0.219978	0.432508	-2.291121
A	0.444364	0.055716	-3.189829
B	1.268189	-0.503306	-3.283678
B	1.459310	-1.259428	-2.657776
A	0.965495	-1.656927	-1.884379

B	0.255341	-1.879653	-1.216491
B	-0.653161	-1.783533	-0.809818
A	-1.504582	-1.262869	-0.746650
B	-1.578376	-0.369291	-1.189448
A	-1.557596	0.523631	-1.639172
B	-0.739898	1.066675	-1.830141
B	0.113194	1.559915	-2.000266
A	1.027615	1.166839	-1.903716
B	1.928092	0.747291	-1.789189
A	2.048504	0.042246	-1.090328
B	1.410687	-0.255968	-0.380218
B	0.694872	-0.476615	0.282294
A	-0.074711	-0.632197	0.901598
B	-0.858279	-0.013484	0.844884
B	-0.934677	0.677467	0.126029
A	-0.778999	0.418222	-0.827153
B	-0.560743	-0.043843	-1.686720
A	-0.310408	-0.533405	-2.521979
B	0.337372	-1.040818	-3.090234
B	0.770256	-0.531522	-2.346440
A	1.031028	0.081018	-1.600259
B	1.181685	0.761207	-0.882872
B	0.607766	1.578979	-0.926071
A	-0.391078	1.531446	-0.918889
B	-1.367073	1.318376	-0.873801
A	-1.829006	0.501407	-0.528579
B	-1.397912	-0.309658	-0.133193
B	-0.837781	-1.075151	0.183464
A	0.074510	-1.212677	-0.202294
B	0.924085	-1.176072	-0.728487
A	1.540988	-0.860680	-1.449567
B	1.854634	-0.317133	-2.228143
B	1.320831	0.424115	-2.635087
A	0.699667	1.130165	-2.975156
B	-0.300051	1.108245	-2.966151
B	-0.904839	0.382850	-2.637471
A	-1.426102	-0.387277	-2.269794
B	-1.917393	-1.171891	-1.891624
A	-1.532661	-2.027320	-1.544895
B	-0.607225	-2.241704	-1.857312
B	-0.015642	-1.517680	-2.212015
A	0.222705	-0.833229	-1.523018
B	0.419780	-0.197002	-0.777114

S_89 Fibonacci sequence global minimum energy computed by Eq. 1 = -325.578412

A	-0.890676	5.222297	11.293380
B	-1.668704	4.931778	10.736363
B	-2.158498	5.528157	10.100414
A	-1.668164	6.004270	9.370424
B	-1.051123	6.389643	8.684315
B	-0.152088	6.170183	8.305408
A	0.750047	5.925282	7.950197
B	1.538695	5.358181	8.187744

A	0.826827	4.723130	7.887825
B	0.036563	4.606234	7.286312
B	-0.894691	4.884079	7.050588
A	-1.682813	4.670039	7.627694
B	-2.347825	4.340134	8.297708
B	-2.648735	3.820308	9.097229
A	-2.285703	3.421407	9.939301
B	-1.657824	3.205639	10.687106
A	-1.047698	2.438666	10.488372
B	-0.448592	1.679773	10.233127
B	-0.073118	1.635437	9.307356
A	0.175184	2.320731	8.622727
B	0.429502	3.028740	7.963908
A	0.961370	3.773140	8.367617
B	1.461699	4.496864	8.842896
B	1.060899	4.700943	9.736040
A	0.580722	4.800837	10.607502
B	0.051615	4.760676	11.455104
B	-0.206286	3.937065	11.960229
A	0.307527	3.094937	11.796475
B	0.935780	2.921734	11.037992
A	1.503541	2.870146	10.216418
B	2.004594	2.923607	9.352655
B	1.989546	3.553174	8.575855
A	1.817329	4.208172	7.840111
B	1.556098	4.869972	7.137416
B	0.721844	5.407230	7.013423
A	-0.183812	5.670363	7.345912
B	-0.999588	5.548707	7.911342
A	-1.748901	5.296576	8.523683
B	-2.477520	5.020295	9.150407
B	-2.337992	4.467211	9.971765
A	-1.423481	4.092965	10.125423
B	-0.656610	4.211696	9.494699
A	0.233414	4.007857	9.902503
B	1.076682	3.845623	10.414925
B	1.784226	4.498139	10.686219
A	1.493482	5.421480	10.435407
B	0.703605	5.818557	9.968050
B	-0.134302	6.070308	9.483763
A	-0.743820	5.424754	9.023605
B	-0.914901	4.602955	8.480119
A	-0.076806	5.105053	8.266837
B	0.622976	5.476910	8.876777
B	1.522606	5.563877	9.304680
A	2.156608	4.894567	9.692060
B	1.890921	3.930661	9.709134
A	1.058479	3.482964	9.382628
B	0.138880	3.359732	9.009600
B	-0.812989	3.507476	8.741054
A	-1.610013	4.038142	9.029405
B	-1.492645	4.909885	9.505099
B	-0.979113	5.537814	10.089894
A	-0.136436	5.670471	10.611711

B	0.713138	5.769108	11.129872
A	1.235614	4.994903	11.487115
B	0.879173	4.060589	11.489658
B	0.131152	3.711345	10.925309
A	-0.587034	3.420047	10.293368
B	-1.290857	3.148875	9.636790
B	-1.913205	2.998510	8.868630
A	-1.660815	3.509169	8.046727
B	-0.894610	3.973606	7.602627
A	-0.054379	4.003275	8.144040
B	0.339086	4.438247	8.953967
B	0.011977	5.023939	9.695563
A	-0.501837	4.623321	10.454180
B	-0.959711	4.067838	11.148288
A	-0.714692	3.117182	11.338593
B	-0.066216	2.493851	10.901628
B	0.583538	2.018076	10.308790
A	0.927769	2.356424	9.432990
B	1.249645	2.721486	8.559421
B	1.494238	3.149799	7.689523
A	0.878466	3.814968	7.267178
B	-0.065908	3.506738	7.152503
A	-0.606076	2.976902	7.806334
B	-0.954466	2.474637	8.597758
B	-1.161863	2.043503	9.475885
A	-0.346425	2.607860	9.604576
B	0.415302	3.024958	10.100354

S_13 Fibonacci sequence global minimum energy computed by LJ term = -18.264451

A	-1.872515	-0.893300	1.154829
B	-2.731132	-0.568108	0.758563
B	-2.520868	0.363275	1.055738
A	-1.590969	0.182426	1.376019
B	-1.309534	0.775524	0.621679
B	-0.785642	0.122565	0.074705
A	-0.850686	-0.469205	0.878182
B	-1.174009	-1.161829	0.233409
A	-2.165186	-1.224768	0.116772
B	-2.796179	-0.659337	-0.414391
B	-2.608159	0.249817	-0.042793
A	-1.790042	-0.174069	0.345796
B	-1.637280	-0.521693	-0.579308

S_21 Fibonacci sequence global minimum energy computed by LJ term = -38.280724

B	-2.598970	-1.071744	-0.989501
A	-2.555464	-1.832540	-1.637030
B	-3.179306	-2.381891	-1.081124
A	-3.006899	-3.100627	-1.754692
B	-2.258990	-3.762954	-1.710463
B	-1.448311	-3.577823	-1.155012
A	-1.257632	-2.619644	-0.941625
B	-0.956978	-2.301922	-1.840880

A	-1.693473	-1.901240	-2.385884
B	-1.498008	-2.638748	-3.032317
B	-2.233398	-3.230214	-2.701607
A	-2.734630	-2.377477	-2.554629
B	-3.551075	-2.074591	-2.063023
B	-3.307601	-1.117647	-1.904976
A	-2.600028	-1.274972	-2.593879
B	-1.969334	-0.931424	-1.898036
A	-1.564488	-1.608399	-1.283378
B	-2.179463	-2.041624	-0.624500
B	-2.319442	-3.001169	-0.868793
A	-1.967465	-2.733347	-1.765666
B	-1.265945	-3.308704	-2.186183

S_34 Fibonacci sequence global minimum energy computed by LJ term = -75.170999

A	0.472359	2.418285	-0.638095
B	-0.322102	2.299673	-1.233713
B	-0.047300	1.650925	-1.943368
A	0.691744	1.410112	-1.314225
B	0.478766	0.496016	-0.969161
B	-0.167306	0.439314	-0.207994
A	-0.553580	1.238591	0.252382
B	0.290259	1.228340	0.788878
A	0.371417	2.187270	0.517094
B	0.329232	2.937186	1.177280
B	1.087189	3.424014	0.743116
A	1.236341	2.671553	0.101590
B	2.127574	2.239059	0.238152
B	2.271682	2.431017	-0.732612
A	1.412721	2.888905	-0.961792
B	0.950592	3.588052	-0.416237
A	0.206155	3.177982	0.110693
B	-0.407799	3.236765	-0.676456
B	0.371919	3.267500	-1.301832
A	0.730286	2.427743	-1.709729
B	1.608837	1.981712	-1.538835
A	1.389475	1.818740	-0.576900
B	1.491686	0.851222	-0.808113
B	0.968414	0.654887	0.021127
A	0.390090	1.417616	-0.268326
B	-0.318322	1.226465	-0.947748
B	-1.130292	1.717089	-0.631537
A	-0.481968	2.287088	-0.126787
B	-0.645757	2.798181	0.716986
A	-0.449328	1.931999	1.176489
B	0.464218	1.940154	1.583146
B	1.267028	2.344961	1.145395
A	1.267005	1.595162	0.483729
B	2.057765	1.152922	0.060503

S_55 Fibonacci sequence global minimum energy computed by LJ term =
-137.241642

B	1.373813	0.169900	-0.003080
A	0.839574	0.156997	-0.848314
B	1.224370	0.867832	-1.437077
A	0.377357	0.770842	-1.959722
B	-0.189950	1.593290	-2.001428
B	-0.752958	1.436535	-1.189978
A	-0.408800	1.311824	-0.259385
B	-1.308185	0.916183	-0.073446
A	-0.858252	0.037826	-0.234832
B	-1.284447	-0.789417	0.131262
B	-0.695297	-1.273802	-0.515477
A	-0.006945	-0.549511	-0.555161
B	0.858993	-0.783863	-0.113315
B	0.673085	-0.297359	0.740354
A	-0.288062	-0.478856	0.532380
B	0.025050	-1.402222	0.310224
A	0.334731	-1.623659	-0.614471
B	-0.271404	-2.223190	-1.137120
B	-1.125174	-1.780380	-1.410972
A	-1.487109	-1.038236	-1.975084
B	-1.530026	-0.039385	-1.996363
A	-0.665714	0.460180	-1.938074
B	-1.205005	1.252159	-2.224309
B	-1.998532	0.927871	-1.709381
A	-1.323163	0.539623	-1.082374
B	-1.904416	-0.024012	-0.495467
B	-1.661492	-0.902707	-0.906419
A	-0.844182	-0.435675	-1.243885
B	-0.228644	-1.185260	-1.487269
A	0.415769	-0.978629	-2.223498
B	0.308049	-1.404688	-3.121756
B	-0.235283	-0.595015	-3.343612
A	0.259806	0.006437	-2.716602
B	1.061168	-0.536598	-2.967464
B	1.955183	-0.345303	-2.562321
A	1.681263	-1.004307	-1.861835
B	1.202204	-1.648374	-2.458224
A	0.675894	-1.879328	-1.639899
B	-0.125260	-1.963959	-2.232342
B	-0.771985	-1.419525	-2.766510
A	-0.580275	-0.552099	-2.307364
B	-0.939675	0.136461	-2.937217
A	-0.345111	0.937011	-2.862293
B	0.600021	1.261688	-2.898470
B	1.277340	0.561780	-2.671830
A	1.081183	-0.097319	-1.945809
B	1.974153	0.069299	-1.527669
B	1.666049	-0.570189	-0.823307
A	0.795558	-0.858027	-1.222548
B	0.130805	-0.203018	-1.581805
A	-0.201357	0.515911	-0.971229
B	0.326022	1.360430	-1.064280

B	0.837993	1.095576	-0.247129
A	0.201303	0.373024	0.022210
B	-0.534534	0.612033	0.655785

S_89 Fibonacci sequence global minimum energy computed by LJ term =
-242.825509

A	0.262401	4.242779	8.095651
B	1.068432	4.121103	7.516420
B	0.659709	3.332733	7.056616
A	-0.176719	3.349537	7.604434
B	-1.092642	3.300990	7.206027
B	-0.785156	4.044326	6.611969
A	0.099885	4.260447	7.024268
B	0.580675	5.096724	7.287862
A	1.005547	5.043997	8.191578
B	1.610226	4.300315	8.476709
B	1.707206	3.305931	8.519077
A	0.790503	3.287169	8.119952
B	0.917618	2.416369	7.645033
B	-0.020586	2.336864	7.308208
A	-0.820510	2.488857	7.888742
B	-1.047035	3.375591	8.291715
A	-0.135793	3.408852	8.702235
B	0.110602	2.490435	8.392721
B	0.127264	1.999318	9.263654
A	-0.024691	2.898665	9.673627
B	-0.906480	3.115770	10.092323
A	-1.040584	3.705501	9.295941
B	-1.951092	3.357325	9.072896
B	-1.708706	2.545623	8.541497
A	-0.829295	2.606496	9.013652
B	-0.838998	2.075203	9.860784
B	-0.099781	2.182613	10.525629
A	-0.039922	3.167379	10.688878
B	-0.649078	3.759855	11.216037
A	-0.886562	4.157247	10.329651
B	-1.805176	3.938417	10.000617
B	-2.328988	4.370486	9.266494
A	-1.628394	4.257806	8.561887
B	-1.998209	3.625284	7.881336
B	-1.661353	4.286907	7.211425
A	-0.799669	4.226626	7.715275
B	-0.551235	5.086298	7.268911
A	-0.073144	5.290318	8.123196
B	0.571077	6.037373	7.959217
B	0.517272	6.824111	8.574157
A	0.401977	6.758480	9.565318
B	1.204549	6.162898	9.531305
A	0.617416	5.492169	9.984507
B	0.713704	6.080373	10.787467
B	-0.234202	6.389185	10.865619
A	-0.345923	5.994866	9.953464
B	-0.724722	6.652212	9.302000
B	-0.402554	6.266276	8.437558

A	0.307962	5.836758	8.994945
B	0.333013	4.837120	9.004377
A	-0.571119	4.495350	8.747993
B	-1.120092	5.123399	8.196463
B	-1.849419	5.310010	8.854684
A	-1.339882	4.756065	9.513103
B	-2.071029	4.998725	10.150706
A	-1.718019	4.498096	10.941120
B	-0.872181	4.798858	11.381687
B	0.077675	4.558385	11.581548
A	0.182024	4.230095	10.642753
B	1.108881	3.982703	10.925125
B	1.911000	4.295324	10.416331
A	1.632244	5.247700	10.292738
B	0.902394	5.026502	10.939569
A	-0.052887	5.286314	10.798382
B	-0.303312	5.670244	11.687135
B	-1.181011	5.874377	11.253575
A	-1.080298	5.286839	10.450671
B	-1.417309	5.856847	9.701329
B	-0.703314	5.492788	9.103273
A	-0.296294	4.909130	9.805896
B	-0.038124	3.964528	9.603241
A	0.775288	3.919465	9.023301
B	1.664446	3.811010	9.467861
B	2.195119	4.657098	9.417666
A	1.314974	5.095290	9.235099
B	0.926354	4.483003	9.923632
A	0.806105	3.497458	10.042964
B	1.700779	3.211873	10.386473
B	1.777215	2.716025	9.521436
A	0.879318	2.857280	9.104515
B	1.042755	1.975180	8.662719
B	1.157882	1.628993	9.593793
A	0.871987	2.423081	10.130158
B	0.909424	2.861616	11.028093
A	0.419355	3.524880	11.593702
B	-0.266002	2.803327	11.691918
B	-0.983369	2.604411	11.024224
A	-1.597429	3.379182	10.873698
B	-1.932869	2.849475	10.094665

S_13 Optimized sequence global minimum energy computed by LJ term =
-18.610603

A	1.038830	-0.765684	0.479799
A	1.015785	-0.076582	-0.244499
B	0.669287	-0.248282	-1.166702
B	-0.056089	-0.909581	-0.975615
A	0.055459	-0.625012	-0.023471
B	0.255497	-1.586615	0.164427
B	1.221177	-1.841911	0.212231
B	1.814616	-1.696593	-0.579420
A	1.903484	-0.763329	-0.231396
B	1.786908	-0.246508	-1.079514

B	1.376632	-1.087295	-1.432712
A	0.902306	-1.121712	-0.553038
B	0.741207	-2.082997	-0.776590

S_21 Optimized sequence global minimum energy computed by LJ term = -39.650163

B	-1.168606	-0.122705	-2.808934
A	-1.862785	0.435824	-2.354887
A	-2.028844	0.286177	-1.380195
B	-2.208717	0.787195	-0.533660
B	-2.321778	1.581406	-1.130690
A	-2.688791	1.008135	-1.863261
B	-3.071911	0.417466	-1.153099
A	-2.710029	-0.513141	-1.098203
B	-1.740871	-0.628266	-0.880305
B	-1.228007	0.201424	-0.659886
B	-1.321287	1.055575	-1.171476
B	-1.642009	1.469229	-2.023548
B	-2.236188	1.350234	-2.819030
A	-2.846012	0.559679	-2.875036
A	-2.806989	-0.083118	-2.109995
A	-1.972821	-0.621171	-1.988909
B	-1.118503	-0.184810	-1.706544
B	-0.832964	0.693723	-2.089489
B	-1.179475	1.016090	-2.970403
B	-1.880494	0.483777	-3.444972
A	-2.235819	-0.357323	-3.037179

S_34 Optimized sequence global minimum energy computed by LJ term = -77.919140

A	-1.545522	1.177180	0.136790
B	-1.852461	0.277788	-0.174471
B	-2.305021	-0.428425	0.370003
B	-3.101351	0.175172	0.330931
A	-3.195326	0.957649	0.946476
B	-4.038946	1.291080	1.367341
B	-4.224617	1.700988	0.474313
A	-3.255779	1.948018	0.456213
B	-2.867313	2.642656	-0.149237
A	-2.003360	2.160413	-0.004241
A	-1.353174	2.093840	0.752612
B	-0.702807	1.334230	0.756818
B	-1.148185	0.439531	0.790805
A	-2.144132	0.521769	0.827252
B	-2.763715	0.018408	1.429532
B	-3.745329	0.034185	1.239312
B	-4.162410	0.586755	0.517710
B	-3.599110	1.065813	-0.155487
A	-2.615162	1.147361	0.003235
A	-2.300719	1.565377	0.855517
A	-1.531879	1.230223	1.400088
B	-1.698313	0.324516	1.789952
B	-2.423976	0.230089	2.471492
B	-2.808893	1.058299	2.878807

B	-2.591776	1.960076	2.505099
A	-2.020424	2.161472	1.709489
A	-2.436276	2.622496	0.925573
B	-3.342021	3.018557	0.774705
B	-3.946384	2.397500	1.273737
A	-3.103517	1.925973	1.533034
B	-3.622960	1.621311	2.331381
B	-3.408948	0.689301	2.038883
A	-2.513309	1.063787	1.798910
B	-1.783385	1.210412	2.466526

S_55 Optimized sequence global minimum energy computed by LJ term = -146.316053

A	-2.973835	0.271336	-0.744174
A	-2.379573	-0.505505	-0.535926
B	-2.754117	-1.430975	-0.592679
B	-3.648686	-1.649556	-0.202848
B	-3.695617	-1.228583	0.703010
A	-3.529803	-0.268431	0.927986
B	-3.858544	0.200964	1.747496
B	-4.795079	0.534182	1.856442
B	-5.226262	1.098880	1.152737
B	-5.657353	0.725177	0.331451
B	-5.332960	-0.127324	-0.078441
A	-4.412782	-0.344033	0.247606
B	-4.467569	-0.661575	1.194267
B	-3.727868	-0.898194	1.824230
B	-2.825390	-0.967957	1.399183
B	-2.667484	-0.976216	0.411764
A	-3.408784	-0.604395	-0.147004
A	-3.362471	-0.704323	-1.140919
B	-2.573241	-0.313214	-1.614362
B	-1.827804	0.182300	-1.168505
A	-2.052405	0.686429	-0.334595
B	-1.634234	-0.087315	0.141275
B	-1.988619	-0.352474	1.037991
B	-2.719519	0.142977	1.507366
A	-3.266001	0.829831	1.028211
A	-2.887597	1.186242	0.173939
B	-3.195715	2.069915	-0.178455
B	-3.631644	2.059588	-1.078376
B	-3.574188	1.270052	-1.689385
A	-3.540737	0.270685	-1.677332
A	-4.301702	-0.377270	-1.710315
A	-5.072404	-0.159082	-1.111640
B	-5.432354	0.717969	-0.793489
A	-4.650887	0.712986	-0.169563
B	-5.035067	1.568016	0.178760
B	-4.598191	2.046878	0.940226
B	-4.142720	1.313925	1.445523
A	-4.369110	0.524691	0.874686
B	-5.225473	0.021948	0.992555
B	-5.377799	-0.910216	0.664122
B	-4.656841	-1.377197	0.152117

A	-4.358333	-0.925402	-0.688582
A	-4.064674	0.028497	-0.750527
A	-4.475313	0.734922	-1.327012
B	-4.626157	1.593895	-0.837716
B	-4.254866	2.224542	-0.156227
A	-3.969040	1.409887	0.348391
B	-3.388986	1.976633	0.933481
B	-2.482623	1.596761	1.118423
B	-2.082081	0.738179	0.798419
A	-2.703822	0.106200	0.335778
A	-3.627577	0.416598	0.111441
A	-3.686799	1.075113	-0.638791
B	-2.761678	1.354487	-0.895892
B	-2.574822	0.783251	-1.695125

s_89 Optimized sequence global minimum energy computed by LJ term = -261.401077

A	5.335687	2.905267	-9.716160
A	5.832940	3.467213	-9.055139
A	6.573647	2.963723	-8.610340
A	6.588762	1.996723	-8.356021
B	5.847304	1.652888	-7.779812
B	5.450839	0.761876	-8.000976
B	5.614742	0.326729	-8.886291
B	6.455216	0.556758	-9.376892
A	6.901018	1.437602	-9.217604
A	7.452963	1.296742	-8.395709
A	8.130765	1.874034	-8.851024
A	7.343220	2.415189	-9.145851
A	7.573687	3.296985	-8.734368
B	8.399980	3.828942	-8.919462
B	7.784366	4.611600	-9.011471
B	6.863774	4.955809	-8.826990
B	5.981103	4.509978	-8.678237
B	6.107616	3.756833	-8.032664
B	5.201538	3.341739	-8.114643
B	4.914555	2.436884	-7.800192
B	4.961990	1.641023	-8.403811
A	5.822732	1.383511	-8.842915
B	6.484006	0.839015	-8.326934
B	6.836661	1.268568	-7.495599
B	6.784960	2.248266	-7.301905
B	6.008944	2.723401	-7.716685
A	5.606019	2.472408	-8.596829
A	6.184722	2.264265	-9.385352
A	6.065528	1.427481	-9.919749
B	5.418240	0.665944	-9.952566
B	4.790851	0.986499	-9.242901
A	5.132237	1.897241	-9.475287
B	4.599280	2.534158	-8.918247
B	4.710900	3.517102	-9.064396
B	5.232536	4.180442	-9.600936
A	5.942526	3.752122	-10.159911
A	6.116817	3.564621	-11.126589

B	5.343402	3.660016	-11.753270
B	5.037800	2.712679	-11.848961
A	5.925344	2.478301	-11.452313
B	6.425150	3.088922	-12.066588
B	6.376102	4.087309	-12.037999
B	5.764629	4.603617	-11.438394
B	6.511205	4.548973	-10.775344
A	6.987514	3.704822	-10.529306
B	7.819385	4.211375	-10.756005
B	8.393817	4.441852	-9.970570
B	8.697227	3.490507	-10.024274
A	8.324763	2.816763	-9.386044
B	8.431279	2.794482	-8.391982
A	7.559624	2.419576	-8.076287
B	7.090471	3.228031	-7.720905
B	7.129588	4.108302	-8.193762
A	6.794454	3.948602	-9.122298
A	6.713603	3.124316	-9.682663
A	6.139630	2.723901	-10.396961
A	5.267798	3.014540	-10.791219
B	4.503855	2.386220	-10.938199
B	4.323784	2.515777	-9.963116
B	4.521673	3.479175	-10.143959
B	5.075225	4.062989	-10.737880
B	5.536667	4.879314	-10.390486
B	6.245523	4.684382	-9.712604
B	7.218278	4.576227	-9.917663
A	7.676200	3.711366	-9.711939
A	7.613535	2.857795	-10.229128
A	6.959172	2.114544	-10.089911
A	6.478405	1.761216	-10.892414
B	6.988109	1.005053	-11.302800
B	7.362086	0.196718	-10.848117
B	7.433998	0.151774	-9.851718
A	7.851979	0.980870	-9.480380
A	7.972920	1.876910	-9.907562
B	8.564523	2.432906	-10.491407
B	8.228152	3.223417	-11.003215
B	7.833432	2.633804	-11.707879
A	7.642734	1.991391	-10.965627
B	7.933594	1.092223	-10.638680
A	7.025067	1.046270	-10.223394
B	6.376887	0.309481	-10.415756
B	5.815884	0.956523	-10.932099
B	4.839685	0.739740	-10.938399
B	4.591087	1.453429	-10.283537
A	5.409067	1.958511	-10.558853
B	5.186689	1.664048	-11.488282
B	6.093856	1.482577	-11.867911
B	6.892296	2.082913	-11.822188
A	6.928889	2.779607	-11.105753
B	7.273290	3.603558	-11.555743

1BDD

REMARK E= -600.67000 Rg= 2.942 SEQ=
 QQNAFYEILHLPNLNEEQRNGFIQSLKDDPSQSANLLAEAKKLNDA

ATOM	RESIDUE	ATOM	X	Y	Z	Occupancy
1	CA	GLN	1	3.800	0.000	0.000
2	CA	GLN	2	3.910	-3.798	0.000
3	CA	ASN	3	2.071	-3.958	-3.321
4	CA	ALA	4	5.026	-2.468	-5.189
5	CA	PHE	5	7.282	-5.270	-3.966
6	CA	TYR	6	4.770	-7.927	-5.000
7	CA	GLU	7	4.137	-6.224	-8.337
8	CA	ILE	8	7.818	-5.337	-8.659
9	CA	LEU	9	8.917	-8.854	-7.732
10	CA	HIS	10	6.631	-10.416	-10.335
11	CA	LEU	11	7.421	-14.129	-10.173
12	CA	PRO	12	4.717	-16.796	-10.045
13	CA	ASN	13	5.064	-17.126	-6.275
14	CA	LEU	14	4.320	-13.433	-5.784
15	CA	ASN	15	1.445	-13.591	-8.265
16	CA	GLU	16	0.065	-16.676	-6.528
17	CA	GLU	17	0.778	-15.102	-3.144
18	CA	GLN	18	-0.955	-11.904	-4.243
19	CA	ARG	19	-4.027	-13.870	-5.309
20	CA	ASN	20	-4.389	-15.441	-1.868
21	CA	GLY	21	-3.735	-12.542	0.501
22	CA	PHE	22	-0.100	-13.473	1.102
23	CA	ILE	23	0.798	-9.982	2.306
24	CA	GLN	24	0.083	-10.849	5.936
25	CA	SER	25	2.002	-14.114	5.625
26	CA	LEU	26	4.650	-12.508	3.425
27	CA	LYS	27	4.868	-9.509	5.748
28	CA	ASP	28	4.984	-11.763	8.805
29	CA	ASP	29	7.472	-14.151	7.210
30	CA	PRO	30	9.863	-11.440	6.038
31	CA	SER	31	8.963	-9.279	3.044
32	CA	GLN	32	12.602	-8.384	2.416
33	CA	SER	33	13.562	-12.061	2.426
34	CA	ALA	34	10.635	-12.926	0.162
35	CA	ASN	35	11.369	-9.894	-2.007
36	CA	LEU	36	15.069	-10.760	-2.004
37	CA	LEU	37	14.261	-14.466	-2.235
38	CA	ALA	38	11.600	-13.778	-4.860
39	CA	GLU	39	13.869	-11.235	-6.541
40	CA	ALA	40	16.883	-13.455	-5.890
41	CA	LYS	41	14.888	-16.512	-6.948
42	CA	LYS	42	13.582	-14.666	-10.002
43	CA	LEU	43	16.977	-13.062	-10.588
44	CA	ASN	44	18.733	-16.411	-10.210
45	CA	ASP	45	16.533	-18.094	-12.811
46	CA	ALA	46	18.211	-16.279	-15.698

1GAB

REMARK E= -680.97900 Rg= 2.382 SEQ=
LLKNAKEDAI AELKKAGITSDFYFNAINKAKTVEEVNALKNEILKAH

ATOM	RESIDUE	ATOM	RESIDUE	X	Y	Z	
1	CA	LEU	1	3.800	0.000	0.000	0.000
2	CA	LEU	2	3.945	-3.797	0.000	0.000
3	CA	LYS	3	0.795	-4.077	-2.106	0.000
4	CA	ASN	4	2.780	-4.504	-5.318	0.000
5	CA	ALA	5	5.485	-6.574	-3.634	0.000
6	CA	LYS	6	2.894	-8.505	-1.635	0.000
7	CA	GLU	7	0.757	-9.029	-4.733	0.000
8	CA	ASP	8	3.821	-10.002	-6.761	0.000
9	CA	ALA	9	5.372	-11.761	-3.771	0.000
10	CA	ILE	10	2.027	-13.341	-2.901	0.000
11	CA	ALA	11	1.446	-14.208	-6.555	0.000
12	CA	GLU	12	5.006	-15.514	-6.807	0.000
13	CA	LEU	13	4.671	-17.056	-3.350	0.000
14	CA	LYS	14	1.267	-18.459	-4.292	0.000
15	CA	LYS	15	2.858	-20.254	-7.239	0.000
16	CA	ALA	16	5.501	-21.762	-4.962	0.000
17	CA	GLY	17	2.853	-23.511	-2.872	0.000
18	CA	ILE	18	3.262	-21.244	0.151	0.000
19	CA	THR	19	0.552	-19.930	2.467	0.000
20	CA	SER	20	-1.303	-16.620	2.252	0.000
21	CA	ASP	21	-1.277	-16.162	6.024	0.000
22	CA	PHE	22	2.504	-16.511	6.163	0.000
23	CA	TYR	23	3.023	-14.360	3.074	0.000
24	CA	PHE	24	0.415	-11.814	4.149	0.000
25	CA	ASN	25	1.440	-11.988	7.803	0.000
26	CA	ALA	26	5.136	-12.204	6.946	0.000
27	CA	ILE	27	4.723	-9.625	4.186	0.000
28	CA	ASN	28	2.376	-7.517	6.305	0.000
29	CA	LYS	29	4.933	-7.369	9.113	0.000
30	CA	ALA	30	7.715	-6.511	6.671	0.000
31	CA	LYS	31	6.169	-3.135	5.863	0.000
32	CA	THR	32	9.260	-1.940	4.003	0.000
33	CA	VAL	33	9.950	-3.126	0.460	0.000
34	CA	GLU	34	13.508	-4.173	1.292	0.000
35	CA	GLU	35	12.244	-6.400	4.100	0.000
36	CA	VAL	36	9.590	-7.832	1.788	0.000
37	CA	ASN	37	12.197	-8.437	-0.909	0.000
38	CA	ALA	38	14.497	-9.993	1.685	0.000
39	CA	LEU	39	11.522	-11.702	3.318	0.000
40	CA	LYS	40	10.319	-12.901	-0.081	0.000
41	CA	ASN	41	13.838	-14.072	-0.912	0.000
42	CA	GLU	42	14.204	-15.525	2.580	0.000
43	CA	ILE	43	10.712	-17.015	2.429	0.000
44	CA	LEU	44	11.242	-18.262	-1.121	0.000
45	CA	LYS	45	14.830	-19.276	-0.388	0.000
46	CA	ALA	46	13.882	-21.129	2.792	0.000
47	CA	HIS	47	11.886	-23.706	0.839	0.000

1LQ7

REMARK E= -936.50600 Rg= 3.321 SEQ=

GSRVKALEEKVKALEEKVKALGGGGRIEELKKKWEELKKKIEELGGGGEVKKVEEEVKKLEEEIKKL

ATOM	1	CA	GLY	1	0.000	0.000	0.000	0.000
ATOM	2	CA	SER	2	3.800	0.000	0.000	0.000
ATOM	3	CA	ARG	3	3.982	-3.796	0.000	0.000
ATOM	4	CA	VAL	4	3.482	-3.977	-3.763	0.000
ATOM	5	CA	LYS	5	5.879	-1.081	-4.317	0.000
ATOM	6	CA	ALA	6	8.391	-2.771	-2.020	0.000
ATOM	7	CA	LEU	7	7.791	-6.057	-3.831	0.000
ATOM	8	CA	GLU	8	8.172	-4.295	-7.177	0.000
ATOM	9	CA	GLU	9	11.222	-2.447	-5.864	0.000
ATOM	10	CA	LYS	10	12.457	-5.655	-4.246	0.000
ATOM	11	CA	VAL	11	11.414	-7.583	-7.350	0.000
ATOM	12	CA	LYS	12	13.174	-5.009	-9.521	0.000
ATOM	13	CA	ALA	13	16.156	-5.156	-7.170	0.000
ATOM	14	CA	LEU	14	15.879	-8.944	-7.058	0.000
ATOM	15	CA	GLU	15	15.297	-9.034	-10.812	0.000
ATOM	16	CA	GLU	16	18.222	-6.663	-11.319	0.000
ATOM	17	CA	LYS	17	20.258	-8.683	-8.826	0.000
ATOM	18	CA	VAL	18	18.966	-11.902	-10.378	0.000
ATOM	19	CA	LYS	19	20.233	-10.816	-13.792	0.000
ATOM	20	CA	ALA	20	23.707	-10.298	-12.343	0.000
ATOM	21	CA	LEU	21	23.558	-13.619	-10.501	0.000
ATOM	22	CA	GLY	22	24.190	-15.603	-13.680	0.000
ATOM	23	CA	GLY	23	21.762	-16.345	-16.508	0.000
ATOM	24	CA	GLY	24	20.899	-19.841	-15.293	0.000
ATOM	25	CA	GLY	25	17.691	-21.761	-14.614	0.000
ATOM	26	CA	ARG	26	16.781	-19.728	-11.536	0.000
ATOM	27	CA	ILE	27	16.678	-16.502	-13.541	0.000
ATOM	28	CA	GLU	28	14.148	-17.973	-15.965	0.000
ATOM	29	CA	GLU	29	11.669	-18.357	-13.110	0.000
ATOM	30	CA	LEU	30	11.908	-14.621	-12.458	0.000
ATOM	31	CA	LYS	31	10.629	-13.896	-15.962	0.000
ATOM	32	CA	LYS	32	7.771	-16.341	-15.427	0.000
ATOM	33	CA	LYS	33	7.277	-14.963	-11.921	0.000
ATOM	34	CA	TRP	34	7.576	-11.445	-13.327	0.000
ATOM	35	CA	GLU	35	4.576	-12.016	-15.588	0.000
ATOM	36	CA	GLU	36	2.720	-13.836	-12.816	0.000
ATOM	37	CA	LEU	37	4.013	-11.407	-10.195	0.000
ATOM	38	CA	LYS	38	3.433	-8.463	-12.528	0.000
ATOM	39	CA	LYS	39	-0.150	-9.566	-13.155	0.000
ATOM	40	CA	LYS	40	-0.568	-10.688	-9.548	0.000
ATOM	41	CA	ILE	41	1.226	-7.600	-8.251	0.000
ATOM	42	CA	GLU	42	-1.395	-5.286	-9.741	0.000
ATOM	43	CA	GLU	43	-4.219	-7.351	-8.259	0.000
ATOM	44	CA	LEU	44	-2.274	-8.073	-5.076	0.000
ATOM	45	CA	GLY	45	-3.151	-4.705	-3.549	0.000
ATOM	46	CA	GLY	46	-3.876	-6.098	-0.089	0.000
ATOM	47	CA	GLY	47	-1.476	-6.606	2.813	0.000
ATOM	48	CA	GLY	48	-2.019	-10.356	3.106	0.000
ATOM	49	CA	GLU	49	-1.503	-11.062	-0.592	0.000
ATOM	50	CA	VAL	50	1.717	-9.044	-0.610	0.000
ATOM	51	CA	LYS	51	3.298	-11.394	1.924	0.000

ATOM	52	CA	LYS	52	3.000	-14.285	-0.524	0.000
ATOM	53	CA	VAL	53	4.909	-12.321	-3.159	0.000
ATOM	54	CA	GLU	54	7.482	-11.280	-0.563	0.000
ATOM	55	CA	GLU	55	7.896	-14.925	0.428	0.000
ATOM	56	CA	GLU	56	7.999	-15.910	-3.240	0.000
ATOM	57	CA	VAL	57	10.249	-12.947	-4.016	0.000
ATOM	58	CA	LYS	58	12.307	-13.610	-0.891	0.000
ATOM	59	CA	LYS	59	12.146	-17.351	-1.538	0.000
ATOM	60	CA	LEU	60	13.132	-16.747	-5.158	0.000
ATOM	61	CA	GLU	61	15.932	-14.430	-4.048	0.000
ATOM	62	CA	GLU	62	16.884	-16.824	-1.254	0.000
ATOM	63	CA	GLU	63	16.557	-19.803	-3.589	0.000
ATOM	64	CA	ILE	64	18.490	-18.002	-6.321	0.000
ATOM	65	CA	LYS	65	21.003	-16.597	-3.840	0.000
ATOM	66	CA	LYS	66	21.936	-20.074	-2.623	0.000
ATOM	67	CA	LEU	67	23.718	-20.892	-5.877	0.000

1CLB

REMARK	E=	-1053.83000	Rg=	2.961	SEQ=			
	KSPEELKGIFEKYAAKEGDPNQLSKEELKLLLQTEFPSLLKGGSTLDELFEELDKNGDGEVSFEEFQVLVKKISQ							
ATOM	1	CA	LYS	1	3.800	0.000	0.000	0.000
ATOM	2	CA	SER	2	3.976	-3.796	0.000	0.000
ATOM	3	CA	PRO	3	3.124	-5.788	-3.122	0.000
ATOM	4	CA	GLU	4	-0.513	-6.749	-3.659	0.000
ATOM	5	CA	GLU	5	-0.003	-10.148	-2.039	0.000
ATOM	6	CA	LEU	6	1.461	-8.549	1.082	0.000
ATOM	7	CA	LYS	7	-1.406	-6.062	1.267	0.000
ATOM	8	CA	GLY	8	-3.999	-8.835	1.108	0.000
ATOM	9	CA	ILE	9	-2.000	-11.228	3.281	0.000
ATOM	10	CA	PHE	10	-1.421	-8.601	5.965	0.000
ATOM	11	CA	GLU	11	-5.040	-7.456	5.787	0.000
ATOM	12	CA	LYS	12	-6.284	-11.043	5.645	0.000
ATOM	13	CA	TYR	13	-3.584	-12.208	8.051	0.000
ATOM	14	CA	ALA	14	-4.184	-9.280	10.397	0.000
ATOM	15	CA	ALA	15	-7.945	-9.587	9.949	0.000
ATOM	16	CA	LYS	16	-7.904	-13.112	11.368	0.000
ATOM	17	CA	GLU	17	-6.120	-11.961	14.519	0.000
ATOM	18	CA	GLY	18	-9.401	-11.106	16.234	0.000
ATOM	19	CA	ASP	19	-11.188	-14.242	15.048	0.000
ATOM	20	CA	PRO	20	-8.781	-16.566	16.850	0.000
ATOM	21	CA	ASN	21	-5.119	-16.591	15.836	0.000
ATOM	22	CA	GLN	22	-5.813	-18.303	12.515	0.000
ATOM	23	CA	LEU	23	-2.978	-16.394	10.854	0.000
ATOM	24	CA	SER	24	-0.829	-19.521	10.635	0.000
ATOM	25	CA	LYS	25	-3.534	-21.447	8.787	0.000
ATOM	26	CA	GLU	26	-4.778	-18.348	6.974	0.000
ATOM	27	CA	GLU	27	-1.231	-17.178	6.272	0.000
ATOM	28	CA	LEU	28	-0.205	-20.714	5.332	0.000
ATOM	29	CA	LYS	29	-3.383	-21.132	3.292	0.000
ATOM	30	CA	LEU	30	-2.955	-17.641	1.851	0.000
ATOM	31	CA	LEU	31	0.777	-18.190	1.391	0.000
ATOM	32	CA	LEU	32	0.177	-21.601	-0.174	0.000
ATOM	33	CA	GLN	33	-2.302	-20.129	-2.650	0.000
ATOM	34	CA	THR	34	0.487	-18.292	-4.464	0.000

ATOM	35	CA	GLU	35	3.508	-20.250	-3.246	0.000
ATOM	36	CA	PHE	36	5.833	-18.729	-0.655	0.000
ATOM	37	CA	PRO	37	9.394	-19.681	0.271	0.000
ATOM	38	CA	SER	38	9.895	-22.379	2.899	0.000
ATOM	39	CA	LEU	39	9.260	-19.969	5.768	0.000
ATOM	40	CA	LEU	40	5.523	-20.647	5.667	0.000
ATOM	41	CA	LYS	41	5.946	-24.112	7.167	0.000
ATOM	42	CA	GLY	42	4.985	-24.665	10.802	0.000
ATOM	43	CA	GLY	43	8.547	-24.681	12.125	0.000
ATOM	44	CA	SER	44	9.508	-21.396	10.473	0.000
ATOM	45	CA	THR	45	9.413	-17.749	11.535	0.000
ATOM	46	CA	LEU	46	5.682	-17.497	10.859	0.000
ATOM	47	CA	ASP	47	4.919	-19.987	13.626	0.000
ATOM	48	CA	GLU	48	7.477	-18.340	15.903	0.000
ATOM	49	CA	LEU	49	6.361	-14.906	14.716	0.000
ATOM	50	CA	PHE	50	2.718	-15.837	15.267	0.000
ATOM	51	CA	GLU	51	3.483	-17.194	18.733	0.000
ATOM	52	CA	GLU	52	6.009	-14.437	19.411	0.000
ATOM	53	CA	LEU	53	3.816	-11.836	17.718	0.000
ATOM	54	CA	ASP	54	0.794	-12.951	19.735	0.000
ATOM	55	CA	LYS	55	2.502	-11.873	22.954	0.000
ATOM	56	CA	ASN	56	2.499	-8.232	21.868	0.000
ATOM	57	CA	GLY	57	-1.036	-7.432	20.729	0.000
ATOM	58	CA	ASP	58	-0.264	-3.878	19.625	0.000
ATOM	59	CA	GLY	59	-0.781	-2.883	15.994	0.000
ATOM	60	CA	GLU	60	2.925	-2.518	15.236	0.000
ATOM	61	CA	VAL	61	3.553	-6.177	16.045	0.000
ATOM	62	CA	SER	62	1.069	-7.290	13.394	0.000
ATOM	63	CA	PHE	63	2.493	-4.819	10.883	0.000
ATOM	64	CA	GLU	64	6.063	-5.580	11.941	0.000
ATOM	65	CA	GLU	65	5.341	-9.311	11.907	0.000
ATOM	66	CA	PHE	66	3.333	-8.942	8.702	0.000
ATOM	67	CA	GLN	67	6.046	-6.766	7.172	0.000
ATOM	68	CA	VAL	68	8.743	-8.965	8.699	0.000
ATOM	69	CA	LEU	69	6.899	-12.147	7.743	0.000
ATOM	70	CA	VAL	70	5.823	-10.668	4.412	0.000
ATOM	71	CA	LYS	71	9.274	-9.208	3.781	0.000
ATOM	72	CA	LYS	72	10.947	-12.381	5.036	0.000
ATOM	73	CA	ILE	73	8.721	-14.570	2.870	0.000
ATOM	74	CA	SER	74	9.364	-12.515	-0.261	0.000
ATOM	75	CA	GLN	75	12.880	-13.884	-0.714	0.000

1E0G

REMARK E= -634.31000 Rg= 2.788 SEQ=

DSITYRVRKGDSLSSIAKRHGVNIKDVMRWNSDTANLQPGDKLTLFVK

ATOM	1	CA	ASP	1	3.800	0.000	0.000	0.000
ATOM	2	CA	SER	2	4.000	-3.795	0.000	0.000
ATOM	3	CA	ILE	3	2.380	-5.979	-2.654	0.000
ATOM	4	CA	THR	4	0.381	-9.176	-2.179	0.000
ATOM	5	CA	TYR	5	0.735	-12.228	-4.416	0.000
ATOM	6	CA	ARG	6	-1.201	-15.467	-4.863	0.000
ATOM	7	CA	VAL	7	0.630	-18.763	-5.330	0.000
ATOM	8	CA	ARG	8	-2.417	-20.557	-6.722	0.000
ATOM	9	CA	LYS	9	-1.398	-19.983	-10.337	0.000

ATOM	10	CA	GLY	10	2.113	-20.872	-11.487	0.000
ATOM	11	CA	ASP	11	2.568	-17.723	-13.566	0.000
ATOM	12	CA	SER	12	2.184	-15.486	-10.519	0.000
ATOM	13	CA	LEU	13	5.898	-14.686	-10.458	0.000
ATOM	14	CA	SER	14	5.846	-13.766	-14.145	0.000
ATOM	15	CA	SER	15	2.516	-11.973	-13.779	0.000
ATOM	16	CA	ILE	16	3.619	-10.353	-10.524	0.000
ATOM	17	CA	ALA	17	7.009	-9.509	-12.020	0.000
ATOM	18	CA	LYS	18	5.327	-8.359	-15.228	0.000
ATOM	19	CA	ARG	19	2.710	-6.425	-13.267	0.000
ATOM	20	CA	HIS	20	5.382	-4.557	-11.315	0.000
ATOM	21	CA	GLY	21	8.134	-3.736	-13.802	0.000
ATOM	22	CA	VAL	22	10.701	-5.987	-12.134	0.000
ATOM	23	CA	ASN	23	12.844	-8.616	-13.847	0.000
ATOM	24	CA	ILE	24	12.715	-12.205	-12.603	0.000
ATOM	25	CA	LYS	25	15.706	-11.687	-10.317	0.000
ATOM	26	CA	ASP	26	14.094	-8.587	-8.822	0.000
ATOM	27	CA	VAL	27	10.802	-10.439	-8.409	0.000
ATOM	28	CA	MET	28	12.634	-13.536	-7.188	0.000
ATOM	29	CA	ARG	29	14.809	-11.381	-4.937	0.000
ATOM	30	CA	TRP	30	11.766	-9.328	-3.954	0.000
ATOM	31	CA	ASN	31	9.690	-12.494	-3.626	0.000
ATOM	32	CA	SER	32	12.348	-14.094	-1.432	0.000
ATOM	33	CA	ASP	33	12.345	-11.133	0.949	0.000
ATOM	34	CA	THR	34	8.569	-10.743	0.782	0.000
ATOM	35	CA	ALA	35	5.761	-12.520	2.626	0.000
ATOM	36	CA	ASN	36	3.977	-15.679	1.496	0.000
ATOM	37	CA	LEU	37	0.468	-16.459	2.729	0.000
ATOM	38	CA	GLN	38	-1.283	-19.820	2.453	0.000
ATOM	39	CA	PRO	39	-5.050	-19.821	1.958	0.000
ATOM	40	CA	GLY	40	-5.222	-23.329	0.508	0.000
ATOM	41	CA	ASP	41	-3.098	-22.329	-2.480	0.000
ATOM	42	CA	LYS	42	-0.516	-19.743	-1.442	0.000
ATOM	43	CA	LEU	43	-0.723	-15.961	-1.129	0.000
ATOM	44	CA	THR	44	2.484	-13.950	-1.462	0.000
ATOM	45	CA	LEU	45	3.125	-10.504	0.007	0.000
ATOM	46	CA	PHE	46	5.520	-8.402	-2.064	0.000
ATOM	47	CA	VAL	47	7.592	-5.229	-1.785	0.000
ATOM	48	CA	LYS	48	8.153	-3.212	-4.956	0.000

1IGD

REMARK	E=	-751.76700	Rg=	3.349	SEQ=		
	MTPAVTTYKLVINGKTLKGETTKAVDAETAEKAFKQYANDNGVDGVWTYDDATKTF					VTE	
ATOM	1	CA	MET	1	3.800	0.000	0.000
ATOM	2	CA	THR	2	3.907	-3.799	0.000
ATOM	3	CA	PRO	3	4.933	-5.977	-2.939
ATOM	4	CA	ALA	4	2.295	-6.653	-5.590
ATOM	5	CA	VAL	5	1.617	-9.983	-7.291
ATOM	6	CA	THR	6	0.096	-10.395	-10.749
ATOM	7	CA	THR	7	-1.317	-13.700	-11.983
ATOM	8	CA	TYR	8	-2.312	-14.533	-15.554
ATOM	9	CA	LYS	9	-4.520	-17.533	-16.308
ATOM	10	CA	LEU	10	-5.036	-19.088	-19.737
ATOM	11	CA	VAL	11	-7.874	-21.301	-18.517

ATOM	12	CA	ILE	12	-9.430	-22.386	-15.224	0.000
ATOM	13	CA	ASN	13	-8.434	-25.723	-13.704	0.000
ATOM	14	CA	GLY	14	-9.232	-27.337	-10.358	0.000
ATOM	15	CA	LYS	15	-7.590	-26.055	-7.179	0.000
ATOM	16	CA	THR	16	-4.174	-25.609	-8.781	0.000
ATOM	17	CA	LEU	17	-2.495	-24.057	-11.817	0.000
ATOM	18	CA	LYS	18	-1.890	-25.886	-15.093	0.000
ATOM	19	CA	GLY	19	0.807	-24.591	-17.435	0.000
ATOM	20	CA	GLU	20	1.729	-21.652	-15.209	0.000
ATOM	21	CA	THR	21	4.095	-18.748	-15.846	0.000
ATOM	22	CA	THR	22	5.445	-16.359	-13.216	0.000
ATOM	23	CA	THR	23	6.722	-12.785	-13.403	0.000
ATOM	24	CA	LYS	24	8.627	-11.098	-10.581	0.000
ATOM	25	CA	ALA	25	8.211	-7.612	-12.037	0.000
ATOM	26	CA	VAL	26	5.374	-6.880	-9.617	0.000
ATOM	27	CA	ASP	27	5.202	-10.565	-8.706	0.000
ATOM	28	CA	ALA	28	3.458	-11.613	-11.916	0.000
ATOM	29	CA	GLU	29	2.062	-15.085	-12.576	0.000
ATOM	30	CA	THR	30	0.826	-16.536	-15.863	0.000
ATOM	31	CA	ALA	31	-1.282	-19.694	-16.024	0.000
ATOM	32	CA	GLU	32	-2.234	-21.892	-18.974	0.000
ATOM	33	CA	LYS	33	-4.854	-23.739	-16.933	0.000
ATOM	34	CA	ALA	34	-5.560	-21.575	-13.890	0.000
ATOM	35	CA	PHE	35	-7.402	-22.485	-10.693	0.000
ATOM	36	CA	LYS	36	-11.071	-23.245	-10.058	0.000
ATOM	37	CA	GLN	37	-11.015	-21.236	-6.833	0.000
ATOM	38	CA	TYR	38	-10.117	-18.090	-8.767	0.000
ATOM	39	CA	ALA	39	-13.117	-18.450	-11.071	0.000
ATOM	40	CA	ASN	40	-15.379	-19.272	-8.131	0.000
ATOM	41	CA	ASP	41	-15.010	-15.825	-6.575	0.000
ATOM	42	CA	ASN	42	-16.214	-14.017	-9.693	0.000
ATOM	43	CA	GLY	43	-12.747	-12.774	-10.630	0.000
ATOM	44	CA	VAL	44	-13.178	-13.427	-14.349	0.000
ATOM	45	CA	ASP	45	-13.797	-9.764	-15.151	0.000
ATOM	46	CA	GLY	46	-10.770	-9.504	-17.433	0.000
ATOM	47	CA	VAL	47	-8.235	-9.251	-14.614	0.000
ATOM	48	CA	TRP	48	-8.376	-10.560	-11.049	0.000
ATOM	49	CA	THR	49	-6.792	-9.100	-7.919	0.000
ATOM	50	CA	TYR	50	-5.401	-10.759	-4.795	0.000
ATOM	51	CA	ASP	51	-4.779	-8.865	-1.560	0.000
ATOM	52	CA	ASP	52	-2.812	-11.693	0.045	0.000
ATOM	53	CA	ALA	53	0.488	-10.010	-0.806	0.000
ATOM	54	CA	THR	54	-1.279	-7.586	-3.139	0.000
ATOM	55	CA	LYS	55	-1.927	-10.046	-5.962	0.000
ATOM	56	CA	THR	56	-3.399	-9.523	-9.426	0.000
ATOM	57	CA	PHE	57	-4.823	-12.297	-11.599	0.000
ATOM	58	CA	THR	58	-5.246	-12.124	-15.371	0.000
ATOM	59	CA	VAL	59	-7.069	-14.532	-17.677	0.000
ATOM	60	CA	THR	60	-6.253	-15.266	-21.315	0.000
ATOM	61	CA	GLU	61	-8.641	-16.763	-23.864	0.000